Platelets

ISSN: 0953-7104 (Print) 1369-1635 (Online) Journal homepage: https://www.tandfonline.com/loi/iplt20

Antiplatelet activity of astaxanthin in control- and high cholesterol-fed rats mediated by down-regulation of $P2Y_{12}$, inhibition of NF-κB, and increasing intracellular levels of cAMP

Huda H. Satti, Eman F. Khaleel, Rehab M. Badi, Amany O. Elrefaie & Dalia G. Mostafa

To cite this article: Huda H. Satti, Eman F. Khaleel, Rehab M. Badi, Amany O. Elrefaie & Dalia G. Mostafa (2020): Antiplatelet activity of astaxanthin in control- and high cholesterol-fed rats mediated by down-regulation of $P2Y_{12}$, inhibition of NF-κB, and increasing intracellular levels of cAMP, Platelets, DOI: 10.1080/09537104.2020.1756237

To link to this article: https://doi.org/10.1080/09537104.2020.1756237

Published online: 07 May 2020.

platelets

http://www.tandfonline.com/iplt
ISSN: 0953-7104 (print), 1369-1635 (electronic)

Platelets, Early Online: 1–10
 DOI: https://doi.org/10.1080/09537104.2020.1756237

Taylor & Francis
Taylor & Francis Group

ARTICLE

Check for updates

Antiplatelet activity of astaxanthin in control- and high cholesterol-fed rats mediated by down-regulation of $P2Y_{12}$, inhibition of NF-κB, and increasing intracellular levels of cAMP

Huda H. Satti[1,2], Eman F. Khaleel[3,4], Rehab M. Badi[3,5], Amany O. Elrefaie[1,6], & Dalia G. Mostafa[3,7]

[1]Department of Pathology, College of Medicine, King Khalid University, Abha, Kingdom of Saudi Arabia, [2]Department of Pathology, University of Khartoum, Khartoum, Sudan, [3]Department of Medical Physiology, College of Medicine, King Khalid University, Abha, Kingdom of Saudi Arabia, [4]Faculty of Medicine, Department of Medical Physiology, Cairo University, Cairo, Egypt, [5]Faculty of Medicine, Department of Physiology, University of Khartoum, Khartoum, Sudan, [6]National Liver Institute, Department of Pathology, Menoufyia University, Menoufyia, Egypt, and [7]Faculty of Medicine, Department of Medical Physiology, Assiut University, Assiut, Egypt

Abstract

This study evaluated the antiplatelet effect of the plant carotenoid, astaxanthin (ASTX) in rats fed either control or high cholesterol plus cholic acid diet (HCCD) and possible underlying mechanisms. Adult male Wistar rats were divided into four groups (n = 8/each), namely, control (fed normal diet), control + ASTX (10 mg/kg/day), HCCD-fed rats, and HCCD + ASTX-treated rats. Diets and treatments were orally administered daily for 30 days. In both control and HCCD-fed rats, ASTX significantly increased fecal levels of triglycerides and cholesterol, reduced platelet count, prolonged bleeding time, and inhibited platelet aggregation. It also reduced platelet levels of reactive oxygen species (ROS) and Bcl-2; thromboxane B2 (TXB2) release; and the expression of $P2Y_{12}$, *P*-selectin, and CD36 receptors. Moreover, the activity NF-κB p65 and Akt was inhibited. Concomitantly, it increased the protein levels of cleaved caspase-3 and vasodilator-stimulated phosphoprotein (*p*-VASP) as well as intracellular levels of cAMP. However, in HCCD-fed rats, the effects of ASTX were associated with reduced serum levels of ox-LDL-c and fasting plasma glucose levels. In conclusion, antiplatelet effects of ASTX involve ROS scavenging, inhibiting NF-κB activity, down-regulating $P2Y_{12}$ expression, and increasing intracellular levels of cAMP that are attributed to its antioxidant, hypolipidemic, and anti-inflammatory effects.

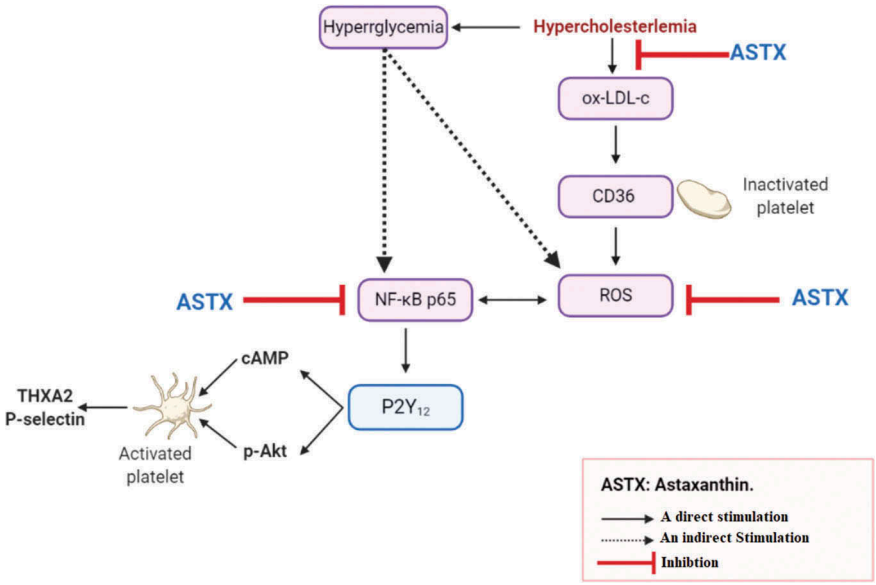

Keywords

Astaxanthin, NF-κB inhibition, P2Y12 down-regulation, platelet aggregation

History

Received 27 December 2019
Revised 31 March 2020
Accepted 10 April 2020
Published online xx xxx xxxx

Correspondence: Huda H. Satti, Department of Pathology, College of Medicine, King Khalid University, P.O.box 3340, Abha 61421, Saudi Arabia. E-mail: hudasatti2010@yahoo.com

Introduction

Hemostasis is a highly regulated process that prevents excessive blood loss and spontaneous thrombosis[1]. It is a tightly controlled mechanism that is regulated by the delicate balance between pro-thrombotic and anti-thrombotic modulators, where a mild disturbance leads to either excessive bleeding or thrombosis[1]. Platelets, the major master regulator of hemostasis, are activated in response to vascular injury[2]. Once stimulated, platelets can change their shape and express multiple surface receptors, which in turn stimulate several intracellular signaling cascades[2]. This leads to degranulation, aggregation, and plug formation[2]. The most common mediators, released from platelets during their activation, are 5-hydroxytryptamine, thromboxane A2 (TXA2), and adenosine diphosphate (ADP)[2].

The $P2Y_{12}$ receptors and G_i-coupled receptors are distributed on the platelet surface and play an important role in the process of platelet activation and aggregation [3–5]. Stimulation of $P2Y_{12}$ receptors by ADP induces rapid activation of the glycoprotein IIb/IIIa receptors (integrin $\alpha_{IIb}\beta_3$) and stimulates platelet degranulation and the expression of surface adhesion molecules [3,4]. In this context, the activation of the $P2Y_{12}$ receptors initiates a cascade of intracellular signaling pathways which ultimately reduces the levels of the secondary messenger, cyclic adenosine monophosphate (cAMP), through the inhibition of adenylyl cyclase[3]. In addition, it potentiates the process of platelet degranulation via the activation of phosphatidylinositol-3kinase/protein kinase B (PI3 K/Akt) signaling pathway [3,5].

Although, platelets are anucleated cells, they have a functional mRNA store, a full protein synthesis system, and multiple transcription factors such as the nuclear factor-kappa B (NF-κB), all of which are activated in response to agonist stimulation [6–8]. Platelets have a complete system required for the activation of NF-κB including; IKK, IκB, and NF-κB p65 subunits[9]. In most cells, including platelets, phosphorylation and degradation of IκB are induced by the phosphorylation of IKK, which leads to phosphorylation and activation of NF-κBp65 to trigger the transcription of numerous genes[7]. In platelets, NF-κB p65 plays a central role in promoting platelet survival, activation, production of inflammatory cytokines, and degranulation[9]. Thrombin, collagen, and ADP agonists can induce NF-κB activation in the platelets[9]. When using washed platelets from healthy volunteers, or experimental rats, pharmacological inhibition of NF-κB by BAY 11–7082 and Ro 106–9920 prevented platelet activation by several mechanisms including; reducing the binding of PAC-1 and fibrinogen to integrin $a_{IIb}\beta_3$, ATP release, ERK phosphorylation, cPLA2 activity, TXB2 synthesis, and *P*-selectin expression, as well as by increasing cAMP and VASP [10,11] Interestingly, recent evidence has shown that $P2Y_{12}$ promoter contains a NF-κB binding site[12]. In a recent study, it was shown that hyperglycemia can trigger platelet activation and aggregation through the up-regulation of $P2Y_{12,}$ and involves activation of NF-κB[12]. However, the mechanisms by which hyperglycemia induces activation of NF-κB in platelets is still unclear.

Nonetheless, hypercholesterolemia is associated with thrombocytopenia and platelet activation, and is considered a serious risk factor for developing spontaneous thrombosis, atherosclerosis and plaque rupture [13,14]. Extensive research has been conducted to better understand the possible mechanisms by which hypercholesterolemia induces platelet activation. It has been shown that, oxidized low-density lipoprotein (ox-LDL-c) or oxidized phospholipids can act as platelet CD36 ligands to stimulate intracellular ROS generation, platelets activation, TXA2 release, and *P*-selectin expression [13,15]. In addition, hypercholesterolemia can activate platelets through enhancing their adhesion with both the leukocytes and the endothelium, this is mediated by increasing the expression of several adhesive molecules [16,17]. Additionally, signaling through the $P2Y_{12}$ receptor and platelet sensitivity to agonist was shown to be dependent on hypercholesterolemia and cholesterol content in the lipid rafts[18]. Moreover, hypercholesterolemia-induced platelet aggregation is associated with up-regulation and activation of the $P2Y_{12}$ receptors, activation of NF-κB, and increasing intracellular levels of ROS and the production of inflammatory cytokines [14,19,20].

Based on this, it seems reasonable that medications targeting NF-κB and $P2Y_{12}$ can effectively prevent hypercholesterolemia-induced platelet activation and aggregation. Astaxanthin (ASTX), 3,3-dihydroxy-β,β-carotene-4,4-dione, is a pure plant carotenoid found abundantly in green algae; and is currently used as a food additive[21]. In rodents, ASTX is safe when used in amounts of up to 1000 mg/day[22]. Currently, accumulating data has confirmed several health benefits of ASTX, including; antioxidant, anti-inflammatory and hypolipidemic effects [21,23–26]. In addition, ASTX is a potent inhibitor of IKK and NF-κ-B activation [27,28]. The antithrombotic activity of ASTX has been reported in several studies [29,30]. Within this view, ASTX reduced blood coagulation and platelet aggregation and promoted fibrinolysis in high-fat diet (HFD)-fed rats mainly due to antioxidant and hypolipidemic properties[31].

The precise mechanism by which ASTX inhibits platelet aggregation is poorly understood. In this study, we investigated the effects of ASTX on platelet activation and aggregation in rats, fed either normal or diet high cholesterol plus cholic acid diet (HCCD). This was achieved by targeting the effect of ASTX on serum lipid levels and various other platelet factors including; expression levels of CD36, $P2Y_{12}$, and *P*-selectin receptors, intracellular levels of ROS, cAMP, and VASP, as well as the activity of NF-κB.

Materials and Methods

Animals

Healthy adult male Wistar rats (160 ± 10 g) were obtained from the animal facility house at the College of Medicine, King Khalid University (KKU), Abha, Saudi Arabia (KSA). All rats were adapted and fed normal chow diet supplied from Diets Inc. (Bethlehem, PA, USA) (Table I) for one week before the beginning of the experimental procedure. During the adaptation and the

Table I. Composition of control diet used in the current study.

Ingredients	g/Kg
Casein	200
Corn-starch	393
Sucrose	154
Corn-oil	155
Wheat bran/cellulose	50
Mineral mix†	35
Vitamin mix‡	10
Vitamin E acetate (500 IU/g)	0.008
DL-Methionine/L-cystine	3
Choline bitartrate	2.5

†The mineral mixture contained (mg/kg of diet): KCl, 4000; MnSO4H2O, 98; trace elements, 400; CuSO4 3 5H2O, 20; FeSO47H2O, 200; CaHPO4, 17.200; MgO, 420; MgSO4, 2000; Fe2O3, 120; ZnSO4 3 7H2O, 0.16; KI, 0.32; and starch to bring to 35 g (per kg of diet).

‡The vitamin mixture contained (mg/kg of diet): thiamine, 40; paminobenzoic acid, 100; retinol, 12; pantothenic acid, 140; cholecalciferol, 0.125; pyridoxine, 20; riboflavin, 30; cyanocobalamin, 0.1biotin, 0.6; inositol, 300; starch to bring to 10 g (per kg of diet).

experimental periods, all rats were housed in a separate room with well-controlled ambient conditions (12 h light/dark cycle, a temperature of 21 ± 1°C, and humidity of 60%). All procedures including animal feeding, treatment, and surgery were approved by the animal ethical committee, College of Medicine, KKU, Abha, KSA; their regulations follow the guidelines and regulations published by the US National Institutes of Health (NIH publication No. 85–23, revised 1996).

Experimental Design

After the one-week adaptation period, the rats were randomly selected and divided into four groups (n = 8/group) as follows: 1) **A control group**: fed normal diet and received dimethyl sulfoxide (DMSO) (diluted in PBS) as a vehicle; **2) A control + ASTX-treated group**: fed normal diet and received a daily dose of ASTX (10 mg/kg) (Cat. No. SML0982, Sigma Aldrich, UK), dissolved in DMSO, **3) A high cholesterol plus cholic acid diet (HCCD)**: fed diet rich in cholesterol and cholic acid (normal diet supplemented with 4% cholesterol and 1% cholic acid) and received DMSO as a vehicle; and **4) A HCCD + ASTX-treated group**: fed HCCD and concomitantly treated with ASTX (10 mg/kg), dissolved in DMSO. All treatments were conducted orally for 30 consecutive days. The final concentration of DMSO in all treatments was 0.05%.

The treatment regimen of ASTX was adopted from previous studies that showed effective hypolipidemic and fibrinolytic effects of ASTX at this dose when given orally[31]. The use of HCCD to induce hypercholesteremia in rats over a period of 30 days was based on the previous study of Thiruchenduran et al. [32] Accordingly, these authors have shown that a diet rich in cholesterol alone or other types of HFD cannot induce hypercholesterolemia in rodents over such a short period of time, whereas the addition of cholic acid to a diet rich in cholesterol enhances the intestinal absorption of cholesterol and successfully induces hypercholesterolemia within 30 days.

Determination of Bleeding Time (BT)

One day after the last treatment, BT was measured in all experimental rats as previously described by Shatoor et al [33]. The rats were not anesthetized, in order to minimize the effect of the anesthesia on BT and were placed in a plastic cylinder with several openings. BT was measured by cutting off the tip of the tail (2 mm) using disposable surgical blades, and maintaining the tail in isotonic saline solution (pH 7.4/37°C) immediately after the injury. BT was defined as the time from the onset of transection until the bleeding stopped completely, and was expressed in seconds.

Blood and Liver Collection

Directly after BT measurements, all rats were anesthetized with an intraperitoneal (i.p) bolus of sodium pentobarbital (60 mg/kg). The chest was opened, and blood samples were collected directly from the heart; 6 ml was withdrawn in acid citrate dextrose (ACD) blood tubes (1:9, v/v) and used within two hours to prepare platelets rich plasma (PRP). Another 2 ml of blood was collected in plain tubes and centrifuged for 10 minutes at 1000 g to obtain serum, which was later used for determining levels of fasting glucose and insulin, as well as levels of TXB2 and lipids. Additional 100 µl blood samples were collected in 100 µl EDTA tubes (Cat. NO. MVC-E-100, SAI-infusion Technology, India).

Complete Blood Count (CBC) and Serum Levels of Glucose and Insulin

Complete blood count (CBC) was performed on the blood for all the experimental groups, using the Sysmex xp-300^{TM} autoanalyzer (Sysmex Corporation, USA). Fasting serum insulin and blood glucose levels were determined using Cobas 8000 autoanalyzer (Roche Diagnostic, Germany).

Biochemical Measurement in the Serum

Serum levels of TXB2 were measured using an EIA assay kit (900—002, Stressgen, Ann Arbor, MI, USA). Serum levels of cholesterol, triglycerides, low-density lipoprotein (LDL-c), high-density lipoprotein (HDL-c), and very-low-density lipoprotein (VLDL-c) levels were measured using commercially available kits (Human Diagnostics, Germany). Serum levels of ox-LDL-c were measured using a rat's ELISA kit (Cat. NO. MBS2501477, MyBioSource, CA, USA). All procedures were conducted in accordance with the manufacturers' instructions, and all measurements were done using Spectramax M2 plate reader (molecular devices, Ca, USA).

Preparation and Adjustment of PRP

The preparation and adjustment of PRP was performed according to the procedure described by Monteiro et al. [34]. ACD-blood samples were collected and centrifuged within 2 h after collection (200 × *g*, 15 min, 37°C), to obtain PRP. To avoid leukocyte contamination, only the top 75% of the PRP was collected[35]. The remainder of the PRP specimen was centrifuged at 1465 *g* for 20 min at 23°C and used to collect platelet-poor plasma (PPP). Thereafter, 3 ml of PRP was mixed with 3.5 ml of washing buffer (10 mM glucose, 140 mM NaCl, 12.5 mM sucrose, 0.5 mM KCl, and 12 mM trisodium citrate) (pH = 6). The mixture was centrifuged at room temperature at 800 *g* for 15 min, to collect platelets. Platelets were then resuspended in Krebs solution containing 5.6 mM glucose, 1.2 mM KH_2PO_4, 118 mM NaCl, 25 mM $NaHCO_3$, and 7 mM $MgSO_4$ (pH 7.4). The platelet count was adjusted to 3×10^8 platelet/ml in the presence of 1 mM $CaCl_2$. The platelet pellets collected from PRP of all rats were immediately stored at −70°C, and later used for the measurement of some biochemical parameters, as well as for western blotting.

Platelet Aggregation

Platelet aggregation was determined within 2 h after blood collection in the hematology research laboratory of the College of Medicine, King Khalid University, Abha, KSA, using the turbidimetric method, [36] using an automated Lumi-aggregometer (Model 400VS; Chrono-Log). In brief, the instrument was calibrated with the absorbance of PPP as 100% and 0.0% for PRP. Samples (450 µl PRP) were incubated for 5 min before being stimulated with 10 µM ADP and aggregation was measured at 37°C under continuous stirring at 1000 rpm. The maximum percentage of platelet aggregation was calculated as the increase in the transmission light after the addition of ADP. All procedures were performed according to the manufacturer's instructions.

ADP-stimulated TXB2 Release

First, 1 ml of platelet suspension was incubated with 10 µM ADP at 37°C for 5 minutes. Then, 10 µl of ice-cold 10% indomethacin-EDTA was added to terminate the reaction. The samples were subsequently centrifuged at 800 *g* for 10 min at room temperature, to obtain supernatants. Supernatants were used directly to measure levels of TXB2 using a rat's special EIA kit (900–002, Stressgen, Ann Arbor, MI, USA). All measurements were done in accordance with the manufacturer's instructions. Absorbance was read at 450 nm using Spectramax M2 plate reader (molecular devices, Ca, USA).

Biochemical Measurements in Platelets Homogenates

Total levels of ROS and nitrogen reactive species (NRS) in the frozen platelets were determined using a fluorometric kit (Cat. No. STA-347, OxiSelect, Cell Biolabs, Inc. CA, USA). The principle of the test relies on measuring the highly fluorescent oxidized product, 2′, 7′-dichlorodihydrofluorescein (DCF) which develops by the end of the reaction. In the test, a highly reactive specific fluorogenic probe (dichloro-dihydro fluorescin DiOxyQ) (DCFH-DiOxyQ) reacts with free ROS and RNS in the homogenate sample to produce a fluorescent DCF, which can be measured by 480/530 nm excitation/emission using a microplate fluorescence reader (FL600Bio-Tek Instruments, Inc., Winooski, VT, USA). Intracellular levels of cAMP were measured in frozen platelet homogenates using an EIA kit (Cat. No. 581001, Cayman Chemical, USA). Platelet pellets were briefly resuspended in sodium acetate buffer (50 mM; pH 4.0), sonicated, boiled for 4 min, and centrifuged at 8000 *g* for 13 min. The supernatant was then used to measure the level of cAMP.

Measurement of NF-κB Activation

Each individual platelet pellet (3×10^8) was homogenized in 250 µl ice-cold phosphate-buffered saline (PBS, pH7.4) in the presence of protease inhibitor cocktail (Cat. No. P8340 Sigma-Aldrich, MO, USA). Protein levels, in all collected supernatants, were determined using a Pierce BCA Protein Assay Kit (Cat. No.23225, ThermoFisher Scientific). Then, 20 µl (20 µg protein) of the homogenates/sample was used for the determination of NF-κB p65 activation using the Trans AM ELISA kit (Cat. No. 40596, Active Motif, Tokyo, Japan). The principle of this test is based on detecting the amount of p65 bounded to oligonucleotides by specific primary and HRP-secondary antibodies. The activation of p65 was calculated using a standard curve generated with recombinant NF-kB p65 (Cat. No. 31102, Active Motif, Tokyo, Japan), and reading absorbance at 540 nm.

Western Blotting

Frozen platelets were homogenized in 250 µl RIPA buffer (Cat. No. ab171675, Cambridge, UK) in the presence of a 5 µl protease inhibitor cocktail (Cat. No. P8340 Sigma-Aldrich, MO, USA). Protein levels in all samples were measured using a Pierce BCA Protein Assay Kit (Cat. No. 23225, Thermo Fisher Scientific). Equal protein concentrations (40 µg) were separated by electrophoresis using 10–12% SDS–polyacrylamide gel and then transferred onto PVDF membranes (Sigma). Membranes were then blocked with skimmed milk, washed and incubated with primary antibodies against; $P2Y_{12}$ (Cat. No. ab183066, 39 kD, 1:500, Abcam. UK), *p*-Selectin (Cat. No. sc-8419, 140 KD, 1:1000), *p*-VASP (Cat. No. sc-365563, 50 KD; 1:1000), CD36 (Cat. No. sc-7309, 88 KD, 1:1000), Akt (Cat. No. sc-5298, 62 KD, 1:1000), *p*-Akt (Ser^{473}) (Cat. No. sc-293125, 60 KD, 1:1000) (Santa Cruze Biotechnology), NF-κB p65 (Cat. No. 8242, 65 KD, 1:500), *p*-NF-κB p65 (Ser^{536}) (Cat. No. 3033, 65 kD: 1: 500), and GAPDH (Cat. No. 2118, 37KD, 1:2000) (Cell signaling Technology, USA). Membranes were then incubated with HRP conjugated secondary antibody. Bands were developed using a Pierce ECL kit (ThermoFisher, USA, Piscataway, NJ) and scanned on a C-DiGit Blot Scanner (LI-COR, USA). Analysis of band intensities was performed using Image Studio (LI-COR, USA). Band density between gels and stripped blots was normalized using a standard. Each membrane was stripped up to 5 times and the detection of phosphorylated forms was performed first. The expression of each protein was presented relatively, with the reference protein.

Statistical Analysis

Statistical analysis of all measured parameters was conducted in Graph Pad Prism (version 6). All data were analyzed by one-way ANOVA, and the significant differences among different treatments were compared through Duncan's Multiple Range Test. Data are presented as mean ± SD. Values are considered significant when P<0.05.

Results

Changes in Final Body Weights, Blood Indices, and Biochemical Parameters

Fasting levels of serum insulin, RBC's count, hemoglobin (Hb) concentration, and other blood indices (MCV, MCH, MCHC) did not vary between groups for all the treatments (Tables II&3). The administration of ASTX to control diet-fed rats significantly increased fecal cholesterol and triglycerides (Table II), decreased platelet count and prolonged bleeding time (Table III), when compared to rats fed only the control diet. On the other hand, final body weights, fasting blood glucose, triglycerides, cholesterol, vLDL-c, LDL-c, OX-LDL-c, platelet count, and fecal levels of triglycerides and cholesterol were significantly increased, whereas serum levels of HDL-c and bleeding time were significantly decreased in HCCD-fed rats, compared to control rats (Tables II&3). The values

Table II. Final body weights and serum and fecal lipids levels in all experimental groups.

	PARAMETER	Control	Control +ASTX	HCCD	HCCD + ASTX
	Final Body weights	254 ± 13.2	249 ± 9.8	302 ± 12.8$^{***\$\$\$}$	262 ± 8.5$^{\#\#\#}$
Serum	Glucose levels (mg/dl)	103 ± 5.4	107 ± 7.2	148 ± 7.4$^{***\$\$\$}$	112 ± 9.5$^{\#\#\#}$
	Insulin levels	5.4 ± 0.8	5.1 ± 0.8	5.5 ± 1.1	5.3 ± 0.9
	TG (mg/dl)	65 ± 8.1	67 ± 6.4	119 ± 8.3$^{***\$\$\$}$	79.5 ± 8.4$^{*\$\#\#\#}$
	CHOL (mg/dl)	74 ± 7.2	71 ± 7.3	158 ± 10.9$^{***\$\$\$}$	94 ± 8.1$^{*\$\#\#\#}$
	LDL-c (mg/g)	32 ± 4.8	34 ± 0.9	110 ± 12$^{***\$\$\$}$	54 ± 8.4$^{**\$\$\#\#\#}$
	HDL-c (nmol/g)	28 ± 3.6	30 ± 4.5	13 ± 3.1$^{***\$\$\$}$	24 ± 5.2$^{\#\#\#}$
	vLDL-c (mg/g)	12 ± 2.9	12 ± 1.9	36 ± 5.4$^{***\$\$\$}$	18 ± 3.7$^{*\$\#\#\#}$
	Ox-LDL-c (ng/ml)	877 ± 89.7	814 ± 69	1489 ± 142$^{***\$\$\$}$	883 ± 76$^{\#\#\#}$
Feces	CHOL (mg/g)	3.4 ± 0.45	4.3 ± 0.3**	5.6 ± 0.5$^{***\$\$\$}$	7.5 ± 0.95$^{***\$\$\$\#\#\#}$
	TGs (mg/g)	1.4 ± 0.41	1.9 ± 0.5**	1.6 ± 0.3$^{\$\$}$	1.95 ± 0.3$^{**\#\#\#}$

Data are presented as mean ± SD of n = 8 rats/group. *,**,***: vs. control diet-fed rats at $P < 0.05$, 0.01 & 0.001, respectively. $^{\$,\$\$,\$\$\$}$: vs. control diet + Astaxanthin (ASTX)-treated rats at $P < 0.05$, 0.01 & 0.001, respectively. $^{\#\#\#}$: vs. high cholesterol and cholic acid (HCCD)- fed rats diet at $P < 0.001$. CHOL: total cholesterol; TG: total triglycerides; LDL-c Low density lipoproteins cholesterol; HDL-c: high density lipoprotein cholesterol; vLDL-c: very low density lipoprotein cholesterol. ASTX was administered at a final dose of 10 mg/kg, orally for 30 days. Fasting glucose and insulin Cobas 8000 autoanalizer All measurements were performed using colorimetric or ELISA kits.

Table III. Complete blood count (CBC) analysis in all experimental groups.

Parameter	Control	Control + ATSX	HCCD	HCCD + ASTX
RBC's ($X10^6$)/mm^3	7.6 ± 0.6	7.2 ± 0.4	7.8 ± 0.8	7.3 ± 0.43
Platelets ($X10^3$)/mm^3	800 ± 54	546 ± 38***	1300 ± 113$^{***\$\$\$}$	766 ± 75$^{\$\$\$\#\#\#}$
Hb (g/dl)	16.2 ± 1.8	15.7 ± 2.7	16 ± 1.9	16.4 ± 2.1
MCV (fl)	59.4 ± 4.2	57.3 ± 3.9	61.4 ± 4.7	58.9 ± 3.6
MCH (pg)	17.8 ± 1.4	19.4 ± 3.2	17.4 ± 2.5	18.9 ± 3.5
MCHC (g/dl)	35.6 ± 4.8	33.3 ± 3.7	34.8 ± 3.1	33.9 ± 5.3
Bleeding Time (s)	112 ± 8.9	154 ± 12.3***	78 ± 7.6$^{***\$\$\$}$	105 ± 8.7$^{\$\$\$\#\#\#}$

Data are presented as mean ± SD of n = 6 rats/group. ***: vs. control diet-fed rats at $P < 0.001$. $^{\$\$\$}$: vs. control diet + Astaxanthin (ASTX)-treated rats at $P < 0.001$. $^{\#\#\#}$: vs. high cholesterol and cholic acid (HCCD)- fed rats diet at $P < 0.001$. RBC's: Red blood cells; Hb: hemoglobin concentration; MCV: mean cell volume; MCH: Mean cell hemoglobin; MCHC: mean cell hemoglobin concertation. ASTX was administered at a final dose of 10 mg/kg, orally for 30 days. CBC analysis was performed on Sysmex xp-300^{TM} hematological autoanalyzer.

of these parameters were reversed in HCCD + ASTX- treated rats, when compared to HCCD-fed rats (Tables II&3).

Effects of ASTX on Platelet Aggregation, TXB2 Release, ROS Generation, Caspase-3, and cAMP/p-VASP in Both Control and HCCD-fed Rats

As shown in Figure 1A-C, platelet maximum aggregation ratio, serum levels of TXB2, and the amount of TXB2 released from washed platelets after ADP stimulation was significantly increased in HCCD-fed rats, compared to control rats. Concomitantly, levels of ROS and protein levels of Bcl-2 were significantly increased whereas, intracellular levels of cAMP and protein levels of *p*-VASP and cleaved caspase-3 were significantly decreased in the platelets collected from HCDD-fed rats, compared to control rats (Figure 2A-D). Platelet aggregation, serum or release levels of TXB2, and platelet intracellular levels of ROS and protein levels of Bcl-2 were significantly decreased whereas, intracellular levels of cAMP and protein levels of vasodilator-stimulated phosphoprotein (*p*-VASP) and cleaved caspase-3 were significantly increased in platelets from both control diet or HCDD-fed rats co-treated with ASTX, compared to control diet or HCCD-fed rats (Figure 1A-C and 2A-D).

Down-regulatory Effect of ASTX on Protein Levels of $P2Y_{12}$ Receptors, *P*-selectin, CD36 and Its Inhibition of Akt and NF-κB P65 Activation in Platelets of Both Control Diet and HCCD-fed Rats

Protein levels of $P2Y_{12}$, phospho-Akt (Ser^{473}) (Figure 3 A&B), *P*-selectin, and CD36 (Figure 4 A&B), as well as the activity and protein levels of *p*-NF-κB p65 (Ser^{536}) (Figure 5A&B) were significantly increased in the platelets of HCCD-fed rats compared to control diet-fed rats. On the contrary, protein levels of $P2Y_{12}$, phospho-Akt (Ser^{473}), *P*-selectin, CD36, and *p*-NF-κB (Ser^{536}), as well as the activation of NF-κB p65 were significantly decreased in the platelets of both control diet + ASTX and HCCD + ASTX-treated rats compared to their controls (Figure 3A&B, 4A&B, and 5A&B).

Discussion

This study provides the first evidence, in literature, that ASTX exerts anti-platelet activity in both the healthy and HCCD-fed rats, and involves decreasing serum levels of TXB2 as well as; downregulation of $P2Y_{12}$ and *P*-selectin receptors expression, inhibition of Akt, and increasing intracellular levels of cAMP and VASP in rat's platelets. These effects are associated with many platelet events including, decreased expression of CD36 (ox-LDL-c receptors), reduced levels of intracellular ROS, and inhibition of NF-κB. Therefore, the summary of our data suggests that the antiplatelet effect of ASTX is mediated mainly by anti-oxidant effects, and possibly by hypoglycemic and hypolipidemic effects.

In this study, we first validated our HCCD animal model by measuring various biochemical parameters. Accordingly, HCCD-fed rats showed a significant increase in rats' final body weights, and an increase in serum levels of cholesterol, triglycerides, LDL-c, and vLDL-c and ox-LDL-c. These data has been also reported in a similar study using the same animal model and diet[32]. In addition, HCCD-fed rats showed higher fasting blood glucose levels with stable plasma levels of insulin, indicating a type 2 diabetes mellitus (DM) phenotype. While all these metabolic endpoints were reversed in HCCD + ASTX-fed rats, their levels remained unchanged in the serum or plasma of control + ASTX-treated rats. Based on this, we

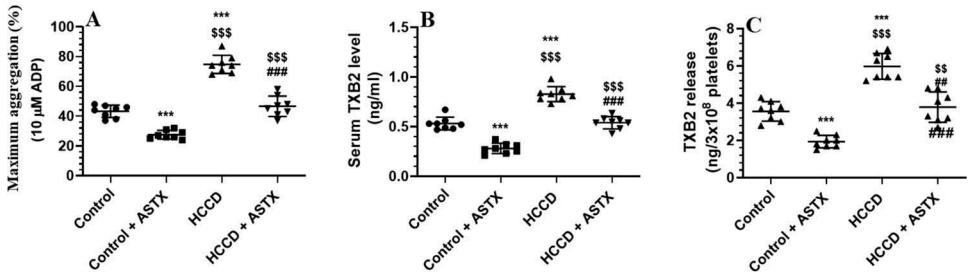

Figure 1. Platelets aggregation (A) induced by 10 µM ADP, serum levels of thromboxane B2 (TXB2) (B) and levels of released TXB2 from washed platelets after stimulation with ADP (10 µM) in all experimental groups. Data are presented as mean ± SD of n = 8 rats/group. ***: vs. control diet-fed rats at $P < .001$. $^{\$\$,\$\$\$}$: vs. control diet + Astaxanthin (ASTX)-treated rats at $P < .01$ & 0.001, respectively. $^{\#\#,\#\#\#}$: vs. high cholesterol and cholic acid (HCCD)- fed rats diet at $P < .01$ & 0.001, respectively. ASTX was administered at a final dose of 10 mg/kg, orally for 30 days. Platelet aggregation was performed using a 400VS automated Lumi-aggregometer. Levels of TXB2 were measured using an EIA kit.

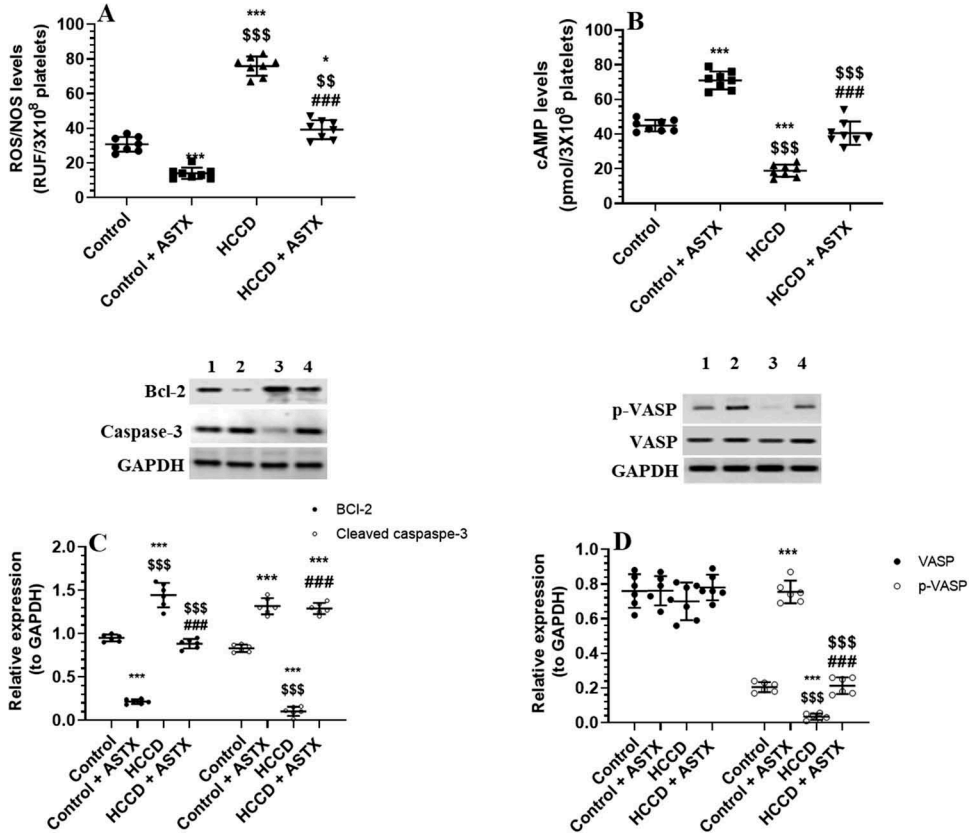

Figure 2. Intracellular levels of reactive oxygen and nitrogen reactive species (ROS/NRS) (A) and cAMP (B), as well as protein levels of Bcl-2, cleaved caspase-3 (C), and *p*-VASP in the platelets of all groups of rats. Data are presented as mean ± SD of n = 8 rats/group. *,***: vs. control diet-fed rats at $P < .05$ & 0.001, respectively. $^{\$\$\$}$: vs. control diet + Astaxanthin (ASTX)-treated rats at $P < .001$. $^{\#\#\#}$: vs. high cholesterol and cholic acid (HCCD)- fed rats diet at $P < .001$, respectively. ASTX was administered at a final dose of 10 mg/kg, orally for 30 days. Platelet intracellular levels of ROS/RNS were measured by measuring using a fluorescent kit based on measuring the 2′,7′-dichlorodihydrofluorescein (DCF). Platelet intracellular levels of cAMP were measured using an EIA kit.

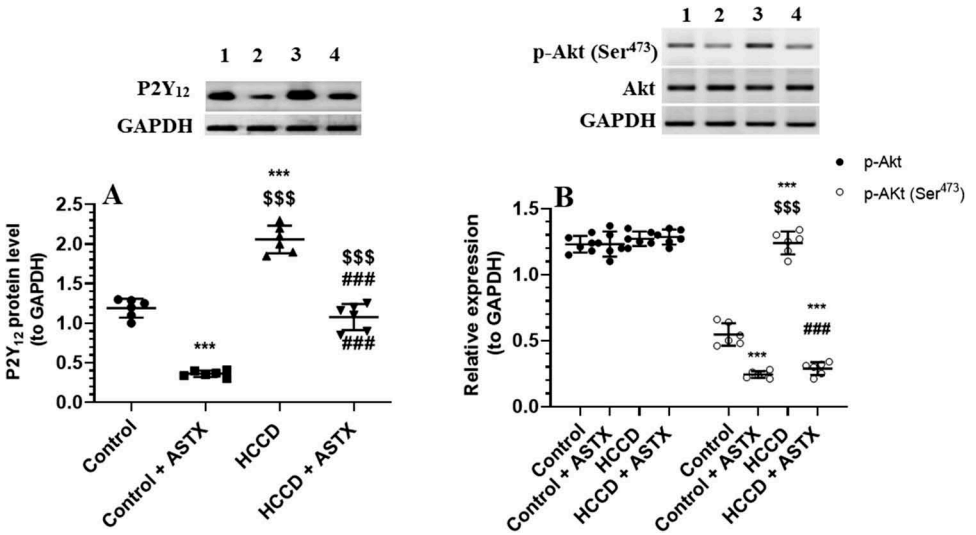

Figure 3. Levels of $P2Y_{12}$ receptors (A) and total/phospho-Akt (Ser473) (B) in the platelets of all groups of rats. Data are presented as mean ± SD of n = 8 rats/group. ***: vs. control diet-fed rats at $P < .001$. $^{\$\$\$}$: vs. control diet + Astaxanthin (ASTX)-treated rats at $P < .001$. $^{\#\#\#}$: vs. high cholesterol and cholic acid (HCCD)- fed rats diet at $P < .001$, respectively. ASTX was administered at a final dose of 10 mg/kg, orally for 30 days. Protein levels were measured using western blotting protocol using 40 µg of each sample/well. Bands were developed using a Pierce ECL kit and scanned on a C-DiGit Blot Scanner. Band intensities were calculated on the accompanied image studio software. Relative expression of each protein was presented as a ratio of the reference protein, GAPDH.

concluded that all the observed hematological effects of ASTX in both control and HCCD-fed rats could be independent of modulating the lipid profile, glucose levels, or food intake. In support, Deng et al. [31] previously showed that ASTX has no effect on the lipid profile in healthy rats but is able to lower serum LDL-c, ox-LDL-c, triglycerides, and cholesterol in HFD-fed rats. Additionally, Ryu

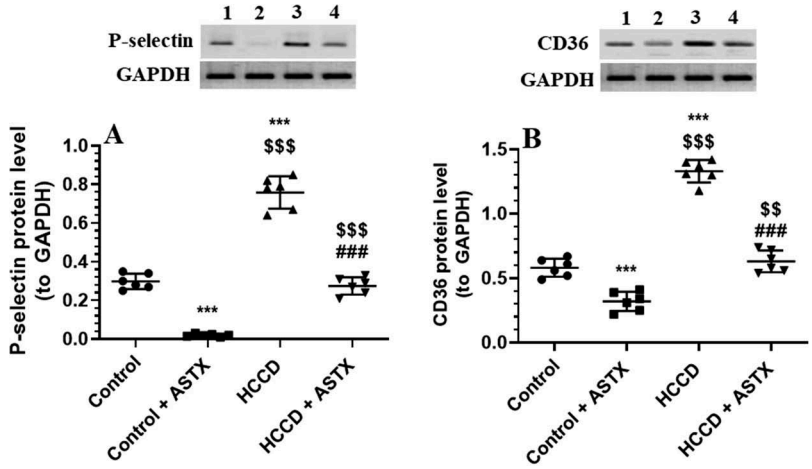

Figure 4. Levels of *P*-selectin (A) and CD36 receptors (B) in the platelets of all groups of rats. Data are presented as mean ± SD of n = 8 rats/group. ***: vs. control diet-fed rats at $P < .001$. $^{\$\$,\$\$\$}$: vs. control diet + Astaxanthin (ASTX)-treated rats at $P < .01$ & 0.001, respectively. $^{\#\#\#}$: vs. high cholesterol and cholic acid (HCCD)- fed rats diet at $P < .001$, respectively. ASTX was administered at a final dose of 10 mg/kg, orally for 30 days. Protein levels were measured using western blotting protocol using 40 µg of each sample/well. Bands were developed using a Pierce ECL kit and scanned on a C-DiGit Blot Scanner. Band intensities were calculated on the accompanied image studio software. Relative expression of each protein was presented as a ratio of the reference protein, GAPDH.

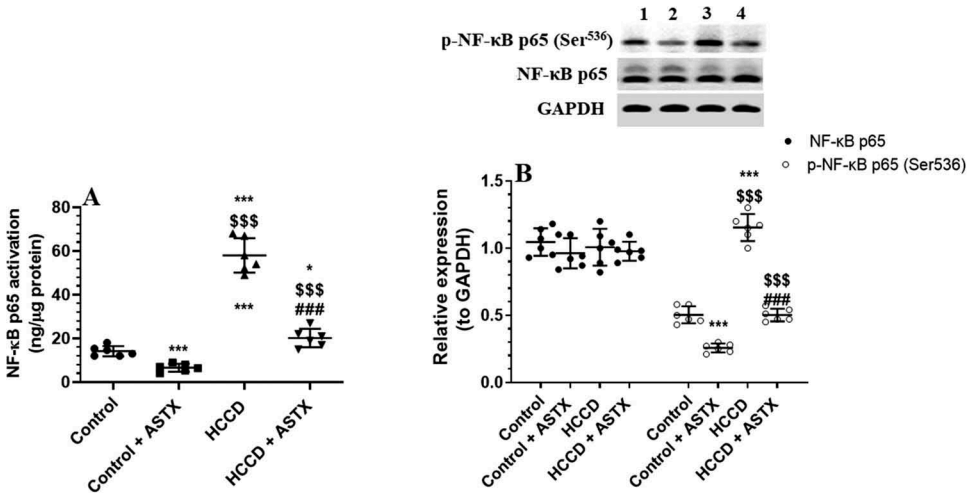

Figure 5. Total activity of NF-κB p65 (A) and protein levels of NF-κB p65 (Ser^{536}) (B)n in the platelets of all groups of rats. Data are presented as mean ± SD of n = 8 rats/group. ***: vs. control diet-fed rats at $P < .001$. $^{\$\$,\$\$\$}$: vs. control diet + Astaxanthin (ASTX)-treated rats at $P < .01$ & 0.001, respectively. $^{\#\#\#}$: vs. high cholesterol and cholic acid (HCCD)- fed rats diet at $P < .001$, respectively. ASTX was administered at a final dose of 10 mg/kg, orally for 30 days. Protein levels were measured using western blotting protocol using 40 µg of each sample/well. Bands were developed using a Pierce ECL kit and scanned on a C-DiGit Blot Scanner. Band intensities were calculated on the accompanied image studio software. Relative expression of each protein was presented as a ratio of the reference protein, GAPDH.

et al., [37] observed that CDX-085, an ASTX pro-drug, significantly reduced serum cholesterol levels in LDL receptors (LDLR)-deficient mice, and reduced serum triglycerides levels in ApoE mice. Similar results were reported in obese animal models[38].

However, the precise mechanisms that trigger the hypolipidemic effect of ASTX remain a matter of debate. In previous studies, this has been linked to increasing ox-LDL-c uptake and fatty acid oxidation, mediated by the upregulation of hepatic carnitine palmitoyl transferase-II (CPT-1) [31,39,40]. In addition to these findings, we show that ASTX increased the fecal levels of cholesterol and triglycerides in both control and HCCD-fed rats, thus suggesting that ASTX may lower serum cholesterol and triglyceride levels by decreasing their intestinal absorption.

On the other hand, Ox-LDL-c and ROS (endogenous or exogenous) play important roles in the activation process of platelet aggregation [15,41]. High levels of ox-LDL-c can increase the platelet production of ROS by acting through CD36 receptors [15]. This has been also demonstrated in HCCD animal models [15,42,43]. Similarly, platelet levels of ROS, and expression of CD36 receptors were significantly increased in HCCD-fed rats of this study, both of which were completely reversed by ASTX treatment. However, with no alteration in ox-LDL-c or in the expression of CD36, ATSX was able to lower the levels of ROS in the platelets of control rats. Such a reduction in platelet levels of ROS in ASTX-treated rats could be explained by the reduction in signaling through the CD36 receptors or due to a direct antioxidant effect of ASTX. Indeed, the antioxidant potential of ASTX was largely attributed to its unique structure that has keto and hydroxyl groups, capable of scavenging ROS [31,44]. In addition, ASTX can stimulate the nuclear factor erythroid 2- related factor 2 (Nrf-2) and heme oxygenase 1 to induce the expression of glutathione and other antioxidant enzymes such as superoxide dismutase (SOD) and glutathione peroxidase (GPx) [31,45,46].

Nonetheless, the process of platelet aggregation is exceptionally complicated and involves different surface receptors, signaling pathways, and intracellular molecules. The cAMP is one of the most intracellular signaling molecules that can inhibit platelet aggregation [11]. Within this view, higher levels of cAMP stimulate the production and phosphorylation of VASP, which inhibits platelet aggregation by inhibiting the binding of fibrinogen to the integrin $\alpha_{IIb}\beta_3$ and reducing TXA2 synthesis and release[11]. In addition, activation of platelet NF-κB transcription factor, which is abundantly inherited in the circulatory platelet, stimulates the process of platelet aggregation by different mechanisms, such as inducing ROS generation,

stimulating Bcl-2-induced platelet survival, and increasing TXA2 synthesis, intracellular levels of cAMP and VASP, *P*-selectin expression, and cPLA2 activity. [9–11,47]

In this study, HCCD increased platelet count, reduced bleeding time, and stimulated platelet aggregation in fed rats. In addition, it concomitantly increased protein levels of Bcl-2, suppressed the expression of cleaved caspase-3, increased the expression of *P*-selectin, and lowered platelets intracellular levels of cAMP and VASP. Interestingly, the platelets from this group of rats also showed an increase in the activity of NF-κB. This suggests that HCCD stimulates cell survival and platelet aggregation, possibly, through activation of NF-κB. However, the exact mechanism by which HCCD induces platelet activation of NF-κB in rats' platelets remains unknown. The cross-talk between ROS and the activation of NF-κB is well established[48]. In addition, hyperglycemia activated NF-κB in the circulatory platelets and megakaryocytes, both *in vivo* and *in vitro*[12]. Therefore, it could be possible that HCCD induces activation of NF-κB in rats platelets by increasing intracellular levels of ROS mediated by activation of ox-LDL-c/CD36 receptor axis, or indirectly due to increasing fasting blood glucose levels as confirmed in the plasma of HCCD-fed rats.

However, not all these effects were seen in the HCCD + ASTX-treated rats. Similarly, ASTX decreased platelet count, inhibited platelet aggregation, reduced platelet expression of Bcl-2 and activity of NF-κB, upregulated platelet cleaved caspase-3, lowered serum levels of TXB2 and increased platelet intracellular levels of cAPM and VASP in control rats. Since fasting plasma glucose and serum ox-LDL-c were not significantly altered in control + ASTX rats, it seems likely that the inhibitory effect of ASTX on the activity of NF-κB is due to the reduction of CD36 and/or an antioxidant effect that reduced levels of ROS. In addition, it could be possible that this is due to a direct anti-inflammatory effect of ASTX, Indeed, the inhibitory effect of ASTX on the activity of NF-κB previously been reported[39].

Nonetheless, hypercholesterolemia can also induce platelet aggregation by increasing the expression and signaling of $P2Y_{12}$ [19]. In general, the binding of ADP to $P2Y_{12}$ receptors promotes the activation of the integrin $\alpha_{IIb}\beta_3$ and intracellular activation of phosphatidylinositol-3 kinase/Protein kinase B (PI3 K/Akt), both of which stimulate degranulation and TXA2 synthesis, and are released to stimulate platelet aggregation [3,49]. In addition, activation of $P2Y_{12}$ receptors leads to the inhibition of platelets adenylyl cyclase (AC) activity and subsequently reduces intracellular levels of cAMP. Similarly [19], we also found a significant increase in the levels of $P2Y_{12}$ receptors with increased Akt activation in the platelets of HCCD-fed rats, which could mediate all events associated with platelet activation. The precise mechanisms by which hypercholesterolemia induces upregulation and activation of $P2Y_{12}$ are still largely unknown. Within this context, recent investigations have shown that the promoter of $P2Y_{12}$ contains an NF-κB binding site and the expression of $P2Y_{12}$ is increased in response to intracellular activation of NF-Kb, induced by hyperglycemia[12]. Hence, it could be possible that HCCD upregulates the platelet $P2Y_{12}$ receptors by increasing the expression of NF-κB through the previously discussed mechanisms. However, another important finding from this study is that ASTX is able to downregulate the expression of $P2Y_{12}$ and inhibit Akt in the platelets of both the control and HCCD-fed rats. These data are the first to show that the antiplatelet effect of ASTX is associated with the downregulation of P2Y12, and inhibition of its intracellular signaling. These effects were associated with the reduction of ROS and inhibition of NF-κB thus, suggesting that ASTX may inhibit $P2Y_{12}$ receptors expression and signaling; via its anti-oxidant and anti-inflammatory effects.

However, in spite of these findings, this study still has some limitations. Firstly, further studies at the molecular level are needed, in order to confirm the connection between ROS, NF-κB and the expression of $P2Y_{12}$ in the platelets of rats after ASTX treatment. In addition, the platelet lipid rafts play an important role in platelet function via the clustering of integrin proteins, regulation of intracellular signaling cascades (e.g., activation of phosphatidylinositol 3-kinase (PIRK)), and expression of surface receptors [50–53]. Hence, it could be possible that ATSX; down-regulates the platelet $P2Y_{12}$ receptors, alters intracellular signaling pathways, and inhibits platelet activation through modulating the phospholipid and cholesterol content of the platelet lipid rafts, an effect that needs further study. Furthermore, it was shown that the impaired cholesterol efflux pathway promotes myelopoiesis and thrombopoiesis [54,55]. In addition, increasing membrane cholesterol levels increases hematopoietic stem and progenitor cell (HSPC) proliferation, and mobilization [56]. The accumulation of cholesterol stimulates the expression of thrombopoietin receptor (c-MPL) on megakaryocyte progenitors, thus increasing the proliferation of megakaryocytes and their differentiation to form platelets[55]. However, if ASTX lowers platelet count and activation by modulating, these events cannot be implied from these data alone and should be considered in future studies.

Conclusion

The results of the current study suggest that ASTX inhibits platelet activation in HCCD as well as in control diet-fed healthy rats. The possible mechanisms include down-regulation of $P2Y_{12}$ and downstream signaling pathways, which ultimately lead to the inhibition of Akt and increasing intracellular levels of cAMP. These effects are associated with reduced serum levels of ox-LDL-c and inhibition of ROS species generation, and NF-κB in rat platelets.

Acknowledgements

The authors wish to thank the technical staff of the animal house at the College of Medicine at KKU for their help in the management, care, and feeding of the animals used in this study. In addition, the authors wish to thank the technical staff at the Department of Biochemistry and the Department of Physiology, College of Medicine at KKU, for their assistance with biochemical measurements.

Disclosure statement

The authors declare that there is no conflict of interest.

Funding

This study is funded by King Khalid University (KKU) through general research project. grant number [188/1440].

Ethical approval

All applicable international, national, and/or institutional guidelines for the care and use of animals were followed.

References

1. Lisman T, Leebeek FWG. Hemostatic alterations in liver disease: a review on pathophysiology, clinical consequences, and treatment. Dig Surg 2007;24:250–258. DOI: 10.1159/000103655
2. Senzel L, Gnatenko DV, Bahou WF. The platelet proteome. Hematol 2009;16(5):329–333.
3. Dorsam RT, Kunapuli SP. Central role of the P2Y12 receptor in platelet activation. J Clin Invest 2004;113(3):340–345. DOI: 10.1172/JCI20986
4. Wallentin L. P2Y12 inhibitors: differences in properties and mechanisms of action and potential consequences for clinical use.

Eur Heart J 2009;30(16):1964–1977. DOI: 10.1093/eurheartj/ehp296
5. Kim S, Kunapuli SP. P2Y12 receptor in platelet activation. Platelets 2011;22(1):54–58.
6. Weyrich AS, Schwertz H, Kraiss LW, Zimmerman GA. Protein synthesis by platelets: historical and new perspectives. J Thromb Haemost 2009;7(2):241–246. DOI: 10.1111/j.1538-7836.2008.03211.x
7. Spinelli SL, Casey AE, Pollock SJ, Gertz JM, McMillan DH, Narasipura SD, Mody NA, King MR, Maggirwar SB, Francis CW, et al. Platelets and megakaryocytes contain functional nuclear factor-kappaB. Arterioscler Thromb Vasc Biol 2010;30:591–598. DOI: 10.1161/ATVBAHA.109.197343
8. Rowley JW, Schwertz H, Weyrich AS. Platelet mRNA: the meaning behind the message. Curr Opin Hematol 2012;19(5):385–391. DOI: 10.1097/MOH.0b013e328357010e
9. Kojok K, El-Kadiry AE, Merhi Y. Role of NF-κB in platelet function. Int J Mol Sci 2019;20(17):4185. DOI: 10.3390/ijms20174185
10. Malaver E, Romaniuk MA, D'Atri LP, Pozner RG, Negrotto S, Benzadón R, Schattner M. NF-jB inhibitors impair platelet activation responses. J Thrombosis Haemostasis 2009;7(8):1333–1343. DOI: 10.1111/j.1538-7836.2009.03492.x
11. Lee HS, Kim SD, Lee WM, Endale M, Kamruzzaman SM, Oh WJ, Cho JY, Kim SK, Cho HJ, Park HJ. Anoble function of BAY 11-7082: inhibition of platelet aggregation mediated by an elevated cAMP-induced VASP, and decreased ERK2/JNK1 phosphorylations. Eur J Pharmacol 2010;627(1–3):85–91. DOI: 10.1016/j.ejphar.2009.11.005
12. Hu L, Chang L, Zhang Y, Zhai L, Zhang S, Qi Z, Yan H, Yan Y, Luo X, Zhang S, et al. Platelets express activated P2Y12 receptor in patients with diabetes mellitus. Circulation 2017;136:817–833. DOI: 10.1161/CIRCULATIONAHA.116.026995
13. Wang N, Tall AR. Cholesterol in platelet biogenesis and activation. Blood 2016;127(16):1949–1953. DOI: 10.1182/blood-2016-01-631259
14. da Motta NA, de Brito FC. Cilostazol exerts antiplatelet and anti-inflammatory effects through AMPK activation and NF-kB inhibition on hypercholesterolemic rats. Fundam Clin Pharmacol 2016;30(4):327–337. DOI: 10.1111/fcp.12195
15. Magwenzi S, Woodward C, Wraith KS, Aburima A, Raslan Z, Jones H, McNeil C1, Wheatcroft S2, Yuldasheva N2, Febbriao M. Oxidized LDLactivates blood platelets through CD36/NOX2-mediated inhibition of thecGMP/protein kinase G signaling cascade. Blood 2015;125(17):2693–2703. DOI: 10.1182/blood-2014-05-574491
16. Libby P, Ridker PM, Hansson GK. Inflammation in atherosclerosis: from pathophysiology to practice. J Am Coll Cardiol 2009;54(23):2129–2138. DOI: 10.1016/j.jacc.2009.09.009
17. von Hundelshausen P, Schmitt MM. Platelets and their chemokines in atherosclerosis-clinical applications. Front Physiol 2014;5:1–17. DOI: 10.3389/fphys.2014.00294
18. Quinton TM, Murugappan S, Kim S, Jin J, Kunapuli SP. Different G protein-coupled signaling pathways are involved in alpha granule release from human platelets. J Thromb Haemost 2004;2(6):978–984. DOI: 10.1111/j.1538-7836.2004.00741.x
19. Nagy BJ, Ashby B, Reilly MP, Kunapuli SP. Contribution of the P2Y12 receptormediated pathway to platelet hyperreactivity in hypercholesterolemia. J Thromb Haemost 2011;9(4):810–819. DOI: 10.1111/j.1538-7836.2011.04217.x
20. Anfossi G, Russo I, Trovati M. Platelet dysfunction in central obesity. Nutr Metab Cardiovasc Dis 2009;19:440–449. DOI: 10.1016/j.numecd.2009.01.006
21. Santos SD, Cahú TB, Firmino GO, de Castro CC, Carvalho LB Jr., Bezerra RS, Filho JLL. Shrimp waste extract and astaxanthin: rat alveolar macrophage, oxidative stress and inflammation. J Food Sci 2012;77(7):H141–6. DOI: 10.1111/j.1750-3841.2012.02762.x
22. Katsumata T, Ishibashi T, Kyle DA. Sub-chronic toxicity evaluation of a natural astaxanthin-rich carotenoid extract of Paracoccus carotinifaciens in rats. Toxicol Rep 2014;1:582–588. DOI: 10.1016/j.toxrep.2014.08.008
23. Park JS, Chyun JH, Kim YK, Line LL, Chew BP. Astaxanthin decreased oxidative stress and inflammation and enhanced immune response in humans. Nutr Metab (Lond) 2010;7:18. DOI: 10.1186/1743-7075-7-18
24. Fassett RG, Coombes JS. Astaxanthin: a potential therapeutic agent in cardiovascular disease. Mar Drugs 2011;9(3):447–465. DOI: 10.3390/md9030447
25. Alam MN, Hossain MM, Rahman MM, Subhan N, Mamun MAA, Ulla A, Reza HM, Alam MA. Astaxanthin prevented oxidative stress in heart and kidneys of isoproterenol-administered aged rats. J Diet Suppl 2018;15(1):42–54. DOI: 10.1080/19390211.2017.1321078
26. Galasso C, Orefice I, Pellone P, Cirino P, Miele R, Ianora A, Brunet C, Sansone C. On the neuroprotective role of astaxanthin: new perspectives mar. Drugs 2018;16:E247.
27. Priyadarshini L, Aggarwal A. Astaxanthin inhibits cytokines production and inflammatory gene expression by suppressing IκB kinase-dependent nuclear factor κB activation in pre and postpartum Murrah buffaloes during different seasons. Vet World 2018;11(6):782–788. DOI: 10.14202/vetworld.2018.782-788
28. Kumar S, Singh SV. Inhibition of NF-κB signaling pathway by astaxanthin supplementation for prevention of heat stress-induced inflammatory changes and apoptosis in Karan Fries heifers. Trop Anim Health Prod 2019;51(5):1125–1134. DOI: 10.1007/s11250-018-01793-y
29. Lauver DA, Driscoll EM, Lucchesi BR. Disodium disuccinateastaxanthin prevents carotid artery rethrombosis and ex vivo platelet activation. Pharmacology 2008;82:67–73. DOI: 10.1159/000132085
30. Khan SK, Malinski T, Mason RP, Kubant R, Jacob RF, Fujioka K, Denstaedt SJ, King TJ, Jackson HL, Hieber AD, et al. Novel astaxanthinprodrug (CDX-085) attenuates thrombosis in a mouse model. Thromb Res 2010;126:299–305. DOI: 10.1016/j.thromres.2010.07.003
31. Deng ZY, Shan WG, Wang SF, Hu MM, Chen Y. Effects of astaxanthin on blood coagulation, fibrinolysis and platelet aggregation in hyperlipidemic rats. Pharm Biol 2017;55(1):663–672. DOI: 10.1080/13880209.2016.1261905
32. Thiruchenduran M, Vijayan NA, Sawaminathan JK, Devaraj SN. Protective effect of grape seed proanthocyanidins against cholesterol cholic acid diet-induced hypercholesterolemia in rats. Cardiovasc Pathol 2011;20(6):361–368. DOI: 10.1016/j.carpath.2010.09.002
33. Shatoor AS, Soliman H, Al-Hashem F, Gamal BE, Othman A, El-Menshawy N. Effect of hawthorn (Crataegusaronia syn. Azarolus (L)) on platelet function in albino Wistar rats. Thromb Res 2012;130(1):75–80. DOI: 10.1016/j.thromres.2012.01.001
34. Monteiro PF, Morganti RP, Delbin MA, Calixto MC, Lopes-Pires ME, Marcondes S, Zanesco A, Antunes E. Platelet hyperaggregability in high-fat fed rats: A role for intra-platelet reactive-oxygen species production. Cardiovasc Diabetol 2012;11:5. DOI: 10.1186/1475-2840-11-5
35. Pignatelli P, Carnevale R, Di Santo S, Bartimoccia S, Sanguigni V, Lenti L, Finocchi A, Mendolicchio L, Soresina AR, Plebani A, et al. Inherited Human gp91 phox deficiency is associated with impaired isoprostane formation and platelet dysfunction. Arterioscler Thromb Vasc Biol 2011;31(2):423–434. DOI: 10.1161/ATVBAHA.110.217885
36. Sheu JR, Lee CR, Lin CH, Hsiao G, Ko WC, Chen YC, Yen MH. Mechanisms involved in the antiplatelet activity of Staphylococcus aureuslipoteichoic acid in human platelets. Thromb Haemost 2000;83:777–784. DOI: 10.1055/s-0037-1613907
37. Ryu SK, King TJ, Fujioka K, Pattison J, Pashkow FJ, Tsimikas S. Effect of an oral astaxanthin prodrug (CDX-085) on lipoprotein levels and progression of atherosclerosis in LDLR (-/-) and ApoE (-/-) mice. Atherosclerosis 2012;222(1):99–105. DOI: 10.1016/j.atherosclerosis.2012.02.002
38. Ikeuchi M, Koyama T, Takahashi J, Yazawa K. Effects of astaxanthin in obese mice fed a high-fat diet. Biosci Biotechnol Biochem 2007;71(4):893–899. DOI: 10.1271/bbb.60521
39. Lee SJ, Bai SK, Lee KS, Namkoong S, Na HJ, Ha KS, Han J-A, Yim S-V, Chang K, Kwon Y-G, et al. Astaxanthin inhibits nitric oxide production and inflammatory gene expression by suppressing I(kappa)B kinase dependent NF-kappa B activation. Mol Cells 2003;16:97–105.
40. Yang Y, Seo JM, Nguyen A, Pham TX, Park HJ, Park Y, Kim B, Bruno RS, Lee J. Astaxanthin-rich extract from the green alga Haematococcuspluvialis lowers plasma lipid concentrations and enhances antioxidantdefense in apolipoprotein E knockout mice. J Nutr 2011;141:1611–1617. DOI: 10.3945/jn.111.142109

41. Vlădăreanu A, Popov V, Radeşi S, Onisâi M, Bumbea H. Role of reactive oxygen species in platelet function in normal states and chronic myeloproliferative disorders. Rom J Biochem 2007;45 (2):221–232.
42. Boullier A, Bird DA, Chang MK, Dennis EA, Friedman P, Gillotre-Taylor K, Hörkkö S, Palinski W, Quehenberger O, Shaw P. Scavenger receptors, oxidized LDL, and atherosclerosis. Ann N Y Acad Sci 2001;947:214–223. DOI: 10.1111/j.1749-6632.2001.tb03943.x
43. Podrez EA, Byzova TV, Febbraio M, Salomon RG, Ma Y, Valiyaveettil M, Poliakov E, Sun M, Finton PJ, Curtis BR. Platelet CD36 links hyperlipidemia, oxidant stress and a prothrombotic phenotype. Nat Med 2007;13(9):1086–1095. DOI: 10.1038/nm1626
44. Choi HD, Kim JH, Chang MJ, Kyu-Youn Y, Shin WG. Effects of astaxanthin on oxidative stress in overweight and obese adults. Phytother Res 2011;25(12):1813–1818. DOI: 10.1002/ptr.3494
45. Motohashi H, Yamamoto M. Nrf2-Keap1 defines a physiologically important stress response mechanism. Trends Mol Med 2004;10:549–557. DOI: 10.1016/j.molmed.2004.09.003
46. Wang HQ, Sun XB, Xu YX, Zhao H, Zhu QY, Zhu CQ. Astaxanthin upregulates heme oxygenase-1 expression through ERK1/2 pathway and itsprotective effect against beta-amyloid-induced cytotoxicity in SH-SY5Ycells. Brain Res 2010;1360:159–167. DOI: 10.1016/j.brainres.2010.08.100
47. Paul M, Kemparaju K, Girish KS. Inhibition of constitutive NF-kappaB activity induces platelet apoptosis via ER stress. Biochem Biophys Res Commun 2017;493:1471–1477. DOI: 10.1016/j.bbrc.2017.10.011
48. Morgan MJ, Liu ZG. Crosstalk of reactive oxygen species and NF-κB signaling. Cell Res 2011;21(1):103–115. DOI: 10.1038/cr.2010.178
49. Kim S, Kunapuli SP. P2Y12 receptor in platelet activation. Platelets 2011;22(1):54. DOI: 10.3109/09537104.2010.497231
50. Rabani V, Montange D, Meneveau N, Davani S. Impact of ticagrelor on P2Y1 and P2Y12 localization and on cholesterol levels in platelet plasma membrane. Platelets 2017;29:709–715. DOI: 10.1080/09537104.2017.1356453
51. Volpe CMO, Villar-Delfino PH, Dos Anjos PMF, Nogueira-Machado JA. Villar-Delfino PH1, Dos Anjos PMF1, Nogueira-Machado JA2. Cellular death, reactive oxygen species (ROS) and diabetic complications. Cell Death Dis 2018;25; 9 (2):119. DOI: 10.1038/s41419-017-0135-z
52. Quinton TM, Kim S, Jin J, Kunapuli SP. Lipid rafts are required in Galphai signaling downstream of the P2Y12 receptor during ADP-mediated platelet activation. J Thromb Haemost 2005;3 (5):1036–1041. DOI: 10.1111/j.1538-7836.2005.01325.x
53. Locke D, Chen H, Liu Y, Liu C, Kahn ML. Lipid rafts orchestrate signaling by the platelet receptor glycoprotein VI. Biol Chem 2002;277(21):18801–18809. DOI: 10.1074/jbc.M111520200
54. Bodin S, Giuriato S, Ragab J, Humbel BM, Viala C, Vieu C, Chap H, Payrastre B. Production of phosphatidylinositol 3,4,5-trisphosphate and phosphatidic acid in platelet rafts: evidence for a critical role of cholesterol-enriched domains in human platelet activation. Biochemistry 2011;40(50):15290–15299. DOI: 10.1021/bi0109313
55. Gomes AL, Carvalho T, Serpa J, Torre C, Dias S. Hypercholesterolemia promotes bone marrow cell mobilization by perturbing the SDF-1: CXCR4axis. Blood 2010;115 (19):3886–3894. DOI: 10.1182/blood-2009-08-240580
56. Morgan PK, Fang L, Lancaster GI, Murphy AJ. Hematopoiesis is regulated by cholesterol efflux pathways and lipid rafts: connections with cardiovascular diseases. J of Lipid Res 2019;jlr.TR119000267.Advance online publication. DOI: 10.1194/jlr.TR119000267